Journal of Materials Chemistry A

ARTICLE

A new layered MWW zeolite obtained by direct synthesis with the bifunctional surfactant template

Received 00th January 20xx,
Accepted 00th January 20xx

DOI: 10.1039/x0xx00000x

www.rsc.org/

Justyna Grzybek,[a] Wieslaw J. Roth,*[a] Barbara Gil,[a] Aleksandra Korzeniowska,[a] Michal Mazur,[b,c] Jiří Čejka,[b,d] and Russell E. Morris[b,c]

The medium pore-size zeolite MWW is very valuable as an industrial catalyst for aromatic alkylation and is the preeminent 2D zeolite: the first identified and the most versatile giving a great variety of novel layered structures and forms, so far about 15 obtained by direct preparation and post-synthesis modifications out of 18 recognised for all layered zeolites. This article reports a new layered MWW layered material, denoted UJM-1P that was obtained by prolonged crystallization of previously reported mono-layered MWW material MIT-1. The latter was synthesised by design using a special bifunctional structure directing agent (SDA) containing adamantyl head group and a long hydrocarbon chain. This was based on the strategy applied 1st to produce layered forms of one of the most important zeolite - MFI. The MWW framework was already known to give 5 different forms by direct synthesis, apparently due to various layer packing, with distinctly different X-ray diffraction patterns. The MFI framework added 3 more types of layered structures by direct synthesis, different from MWW family. Two were prepared with the aforementioned bifunctional SDA, prior to MIT-1, and were composed of novel building units, layers covered with protruding organic parts from the SDA. Since MIT-1 and UJM-1P/1 are analogues of these layered MFI materials, they can considered as the 6th and 7th MWW forms obtained by one-pot preparation process. UJM-1P/1 has distinct structural features revealed by X-ray and electron diffraction and microscopy, especially extensive layer disorder. It also shows unique and particularly facile swelling with surfactants, which indicates weak interlayer connection that may be due to the special SDA molecules lining the surface of its layers. This is promising for delamination and formation of colloidal dispersions of MWW mono-layers. UJM-1 was confirmed to be a very active solid acid catalyst showing high concentration of Brønstead acid sites of about 900 µmol/g. It was tested in the mesitylene alkylation showing activity comparable to MCM-22 and MCM-56, while MIT-1 was about 50% less active.

Introduction

Zeolites are a special class of inorganic materials, initially aluminosilicates, with microporous framework structures[1, 2] that show exceptional activity as heterogeneous catalysts for conversion of organic compounds.[3, 4] The development of zeolites started expansion in a new direction in the 1990s with the surprising discovery that they can form layered structures,[5-7] similar to 2-dimensional solids and thus called 2D zeolites.[8] Originally zeolite frameworks were viewed as exclusively fully connected 3D structures.[9] Zeolite layers are molecularly thin, up to about 3 nm and so far a have been produced by about 20 out of 240 known frameworks.[10, 11] They have been obtained by 3 basic approaches:[12] conventional (zeolite) hydrothermal synthesis usually with organic additives as structure directing agents (SDA),[13] degradation of zeolites with built in weaknesses called ADOR strategy,[14, 15] and by using special bifunctional SDAs with surfactant tails.[16, 17] The last method was invented to synthesize by design the 2nd most important and valuable zeolite ZSM-5/MFI as a layered structure.[16]

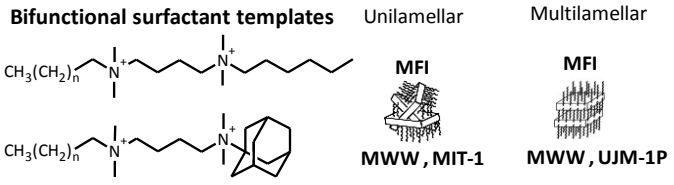

Figure 1. Bifunctional surfactant templates used for the synthesis of MFI and MWW layers by design. N atoms are connected by 4-6 CH_2 groups. The 'n' in the side chain are usually 20 for MFI and 14 for MWW with total length of 22 and 16 carbon atoms.

The bifunctional SDAs, shown in the Fig. 1, consisted of a quaternary ammonium head group templating the framework and a long hydrocarbon tail designed to prevent framework propagation in the 3rd dimension. By using various head

[a] Faculty of Chemistry, Jagiellonian University in Kraków, Gronostajowa 2, 30-387 Kraków, Poland e-mail: wieslaw.roth@uj.edu.pl
[b] Department of Physical and Macromolecular Chemistry, Faculty of Sciences, Charles University, Hlavova 8, 128 43 Prague 2, Czech Republic
[c] EaStCHEM School of Chemistry, University of St Andrews, St Andrews KY16 9ST, UK
[d] J. Heyrovský Institute of Physical Chemistry Academy of Sciences of Czech Republic, v.v.i., Dolejškova 2155/3, 182 23 Prague 8, Czech Republic.
Electronic Supplementary Information (ESI) available: See DOI: 10.1039/x0xx00000x

groups with tails of different length and changing synthesis conditions two basic types of materials were obtained: an apparent house-of-cards structure consisting of mono-layers[18] and multi-layered crystals with interlayer gallery heights of approximately 2-4 nm.[19] These were breakthrough results fundamentally and very promising for catalysis.

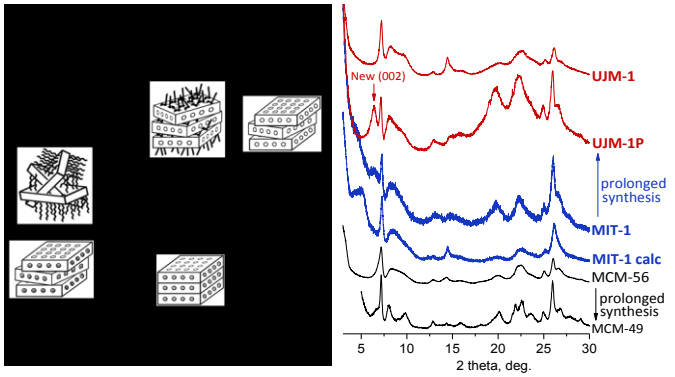

Figure 2. XRD patterns showing transformation of MIT-1 to UJM-1P indicated by the new (002) peak, and its comparison with MCM-56. MIT-1 shows onset of the (002) reflection at 6.5 deg. suggesting possible UJM-1P 'impurity'. The broad peak at ca. 4.5 for calcined MIT-1 is assigned to kenyaite impurity.

This strategy was extended recently to the synthesis of mono-layers of zeolite MWW, which produced a material with the house-of-cards structure, denoted MIT-1 by Leshkov et al..[20] Zeolite MWW contains 2 independent medium size pore channels with large cavities and is an outstanding catalyst used commercially for aromatic alkylation.[21] It provided the initial discovery of layered zeolites[22] and, as elaborated later, has produced several layered forms by direct synthesis, including the mono-layer material designated MCM-56.[23] MIT-1 showed promising activity as catalyst for alkylation in comparison to other MWW forms including layered.[20] We have found that MIT-1 is a transient product. As its crystallization is prolonged a new peak begins to grow in the XRD of the solid product at 6.5 deg. 2-theta as shown in Fig.2. It can be recognised as the (002) reflection characteristic for expanded multi-layered MWW materials, such as MCM-22P and EMM-10P. We denoted this product UJM-1P. Just like these other expanded multilamellar MWW materials it contracts upon calcination to about 2.5 nm, which is indicated by disappearance of the peak at 6.5 deg. 2-theta;[24, 25] the calcined product is named UJM-1. In this case the bifunctional SDA fulfils its role to thwart expansion of the framework structure in the 3rd dimension, but it does not inhibit layer stacking. This is similar to the MFI syntheses except that with UJM-1P the interlayer distance is much smaller.

This report has two objectives. First, specific, is to present the synthesis, properties and catalytic activity of UJM-1P as a new member of the MWW zeolite family. Second, more general, has to do with the fact that because zeolites can grow as layers they can be obtained in different (layered) forms by direct synthesis, as illustrated by MWW and MFI. The conventional zeolites afford only one type of structure – 3D framework extended continuously in all directions with the possible variation of crystal habits. Zeolite MWW was initially obtained by direct synthesis in 5 different forms, clearly distinguishable by visibly different XRD patterns, shown in Fig 2. MFI contributes additional 3 different forms.[11] Thus, various layered zeolites and their different forms that can be synthesised directly represent an important group worth separate attention. They are expected with other topologies besides MWW and MFI but so far have been limited to basically one 2D precursor and the 3D form.[26] The paper proposes formally defined various layered zeolite forms based on recognised differences. It can be used for further analysis and validation, possible expansion into new forms and replication with other topologies. Aside from the fundamental importance, the directly synthesised zeolite materials are significant as potentially more convenient and economical for scale-up and development in clear self-evident preference to more laborious and often expensive post-synthesis modifications.[27]

Experimental

Synthesis

Preparation of the structure directing agent (SDA) - $C_{10}H_{15}$-$N^+(CH_3)_2$-C_4H_8-$N^+(CH_3)_2$-$C_{16}H_{33}$ (Ada-4-16)

The synthesis was carried out in three steps according to the published procedure.[20] In the first step, 1-adamantylamine (15 g, 97 %, Sigma Aldrich) was dissolved in formaldehyde (23.42 g, 37%, Sigma Aldrich) and heated to 373 K under reflux. Formic acid (14 g, 95%, Sigma Aldrich) was added to this mixture dropwise with an addition funnel in the span of 2 hrs. and the mixture refluxed for another 3 hrs. The solution was allowed to cool to room temperature and adjusted to pH = 12 with sodium hydroxide solution (50%, Sigma Aldrich). The product, dimethyl-1- adamantylamine (Ada-N(Me)$_2$), was liquid-liquid extracted from the mixture with diethyl ether and dried with potassium carbonate (99 wt%, Sigma Aldrich). The ether solvent was removed by rotary evaporation. The obtained white solid was dried overnight at room temperature, yield 84%. Its composition as Ada-N(Me)$_2$ confirmed by ^{1}H NMR. Next, 14.48 g of Ada-N(Me)$_2$ and 1,4-dibromobutane (157.9 g, 99%, Sigma Aldrich) were dissolved in 362 ml of acetonitrile (anhydrous 99.8%, Sigma Aldrich) and refluxed at 355 K for 16 h. The solvent was removed by rotary evaporation. The product (Ada-N^+(Me)$_2$-4-Br,Br^-) was recrystallised from dichloromethane and washed with diethyl ether. White solid was obtained with 56% yield. Ada-N^+(Me)$_2$-4-Br,Br^- composition was verified by ^{1}H NMR. 17.97 g of Ada-N^+(Me)$_2$-4-Br,Br^- and N,N-dimethylhexadecylamine (37.39 g, 95%, Sigma Aldrich) were dissolved in 450 ml of acetonitrile, and refluxed at 355 K for 18 h. The solvent was removed by rotary evaporation and the product in bromide form was washed with diethyl ether. Ada-4-16 composition was verified using ^{1}H and ^{13}C NMR. The final product was converted from the bromide to hydroxide form using hydroxide exchange resin

(Ambersep 900 OH, Alfa Aesar) in water and then titrated using HCl to determine OH^- concentration.

Preparation of zeolites

Both MWW materials, MIT-1 and UJM-1P, were obtained from similar mixtures of composition $1SiO_2$/0.1 OSDA/0.05 $Al(OH)_3$/0.2 NaOH/45 H_2O by the standard hydrothermal procedures.

As the first step a weighted amount of the template was dissolved in water and converted to the hydroxide form by mixing with ion exchange resin. The obtained aqueous solution of Ada-4-16 (in hydroxide form) was combined with NaOH (50%, Sigma Aldrich), aluminium hydroxide (Sigma Aldrich), colloidal silica (LUDOX® LS 30) and stirred over 4h at room temperature. The gel was transferred to a Teflon liner, sealed in the pressure bomb and held at 433 K with rotation for 7-10 and 14 days. After crystallization the solids were recovered by filtration, washed with deionised H_2O, and dried at 338 K for overnight.

Solid were calcined by heating under flowing N_2 at a rate of 2 K/min with a 1 h hold at 423 K, a 2 h hold at 573 K, and a 3 h hold at 813 K. The flowing gas was then switched to dry air and the temperature was held at 813 K for another 6 h.

Characterization methods

The structure and crystallinity of obtained zeolites were determined by X-ray powder diffraction (XRD) using a Bruker AXS D8 Advance diffractometer equipped with a graphite monochromator and a position sensitive detector (Våntec-1) using CuK_α radiation in Bragg–Brentano geometry and Rigaku MiniFlex diffractometer in reflection mode, using CuK_α radiation (ʎ = 0.154 nm). The XRD patterns were usually collected with steps of 0.02°.

Nitrogen adsorption isotherms were determined by the standard method at -196 °C (liquid nitrogen temperature) using an ASAP 2025 (Micromeritics) static volumetric apparatus. Before adsorption the samples were outgassed at 350 °C using turbomolecular pump to remove adsorbed water.

TEM images and SAED diffraction patterns were recorded using Titan Themis 200 transmission equipped with an X-FEG Schottky field emission gun at 200 keV. The microscope is equipped with 16 mega-pixel CMOS camera and was aligned using standard gold sample methods.

Relative content of Al and Si was determined in the samples formulated into pellets, 20 mm in diameter, with the use of Energy-Dispersive XRF spectrometer (Thermo Scientific, ARL QUANT'X). The X-rays of 4-50 kV (1 kV step) with the beam size of 1 mm were generated with the Rh anode. The detector used was a 3.5 mm Si(Li) drifted crystal with a Peltier cooling (ca. 185 K). For quantitative analysis, calibration with a series of metallic standards and UniQuant software were used.

The concentration of Lewis (LAS) and Brønsted (BAS) acid sites was determined using adsorption of pyridine (Py) followed by IR spectroscopy (Tensor 27 from Bruker, MTC detector, spectral resolution 2 cm^{-1}). Zeolites were pressed into self-supporting wafers with a density of ca 8 mg/cm^2 and activated in situ at 450°C for 1 hour at high vacuum (10^{-5} mBar). Excess of pyridine vapor was adsorbed at 170 °C followed by desorption for 20 min at 170 °C. Spectra were recalculated to a wafer mass equal 10 mg. Concentration of Lewis (LAS) and Brønsted (BAS) acid sites were evaluated from the intensities of bands at 1454 cm^{-1} (LAS) and at 1545 cm^{-1} (BAS) using absorption coefficients determined earlier in our laboratory using external standards,[28] ε (LAS) =0.165 cm^2/μmol, and ε (BAS) =0.044 cm^2/μmol and the intensities of corresponding pyridine maxima after pyridine desorption at 170°C to ensure complete removal of weakly adsorbed species.

Catalytic testing

Preparation of catalysts

Calcined samples were ion exchanged into NH_4^+ – form, with 1 M solution of NH_4NO_3 (Avantor Poland, p.p.a.) for 1 h at room temperature (20 ml of solution per 0.5 g of zeolite), repeated three times, filtered, washed with deionised water, dried, and activated at 723 K for 5 h.

Catalytic tests

The test reaction - liquid phase benzylation of mesitylene with benzyl alcohol (Figure 3) was carried out in a three-necked round-bottom flask equipped with a reflux condenser with heating in a multi-experiment workstation StarFish (Radleys Discovery Technologies) under atmospheric pressure. The reaction temperature was 353 K. Typically, 130 mmol of mesitylene (15.5 g) was combined with 50 mg catalyst and dodecane as an internal standard. The reaction mixture was maintained for 30 min at the required reaction temperature and then 1 mmol of benzyl alcohol was added. This was regarded as the initial reaction time. Liquid samples were withdrawn at regular intervals and analysed by the gas chromatography Agilent 7820A GC with an FID detector using a 30 m packed DB-5 column. The conversion of alcohol was calculated as following:

$$\text{conversion} = k \cdot \frac{S_{alcohol}}{n_0} \cdot 100\%$$

where S is the area of respective peak in the chromatogram, k is the calibration coefficient (mol), n_0 is the starting amount of alcohol (mol).

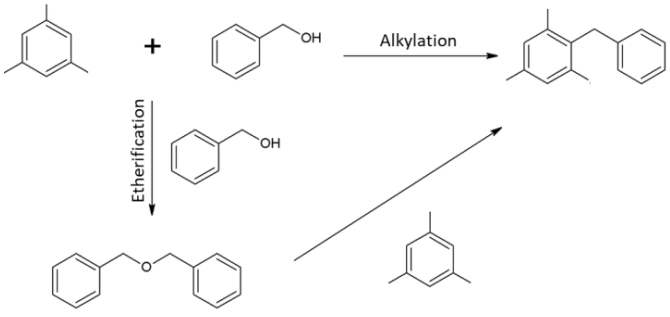

Figure 3. Alkylation of mesitylene with benzyl alcohol.

Results and discussion

Various layered zeolite forms by direct synthesis

The MWW and MFI frameworks provide collectively 8 various layered forms by direct synthesis, not overlapping except for the 3D framework. 5 different layered MWW forms were obtained in the past by slight changes in the synthesis mixture compositions, like changing Al and base content, and sometimes with different templates.[23, 29] They can be clearly differentiated based on visually different XRD patterns, especially in the range 6-10 deg. 2-theta, with various combinations of discrete peaks and broad bands, as shown in the Table 1. This is possible due to fortuitous location of intra- and inter-layer peaks in this range and may not be so easy with other zeolites. The proof that these materials are indeed MWW layers is provided by the characteristic intralayer reflections (100), (220) and (310) at 7.1 (strong), 25 (medium), and 26 (strong) deg. 2-theta. The XRDs can be rationalised starting from the basic MWW zeolite structure (MCM-49, MCM-22 calcined).[22] It shows 3 peaks: one is composed of the overlapping pure interlayer (002) and intralayer (100) and the others are (101) and (102). The expanded MCM-22P layered precursor shows 4 peaks as the (002) is shifted to lower 2-theta (d-spacing >2.6 nm). It is formally recognised as 'layered (zeolite) precursor', a slightly expanded structure, which condenses topotactically with contraction to produce the complete 3D framework[13] with 3 peaks like above. The precursor is the most common and usually the only layered form known with other frameworks (about 20). Sometimes simple calcination does not give an ordered complete framework but often the precursors can be modified by intercalation and then may condense giving a zeolite.[30] The remaining 3 MWW species have broad bands instead of the (101) and (102) peaks, which is interpreted as due to lateral layer disorder.

The known layered forms of ZSM-5/MFI are different from the 4 layered MWW ones discussed above. Unlike MWW, MFI has no comparable XRD features for structure differentiation, so the definitions are based on another evidence. None of the 3 MFI materials is a 'layered MFI zeolite precursor' *sensu stricte*, i.e. condensing into complete framework. Two are recognised as produced from a novel type of building blocks, namely layers incorporating the special bifunctional SDA[16] intended to prevent structure propagation in 3D. As mentioned above they are the unilamellar 'house-of-cards'[18] and multilayered stacks of MFI nanosheets.[16] The 3rd unique product called self-pillared, consists of MFI sheets intergrown at right angles.[31] It is produced due to the ability of MFI and MEL framework to form continuous combinations. Post-synthetic modifications afford additional derivatives,[32] quite valuable, like pillared, delaminated, stabilised precursors and others, but those obtained by one-pot syntheses are particularly significant. As mentioned they are important fundamentally and may be more attractive for practical implementation and therefore deserve special attention.

Table 1. Layered zeolite forms synthesised directly based on MWW and MFI frameworks. Letter 'P' for 'precursor' or uncalcined form is not used universally and consistently in the literature. The (100) reflection for MWW is marked with the red line.

Building blocks	Layered zeolite form - proposed ('→' - change upon calcination)	Structure	XRD-MWW (100)	XRD 6-10°, MWW as-made	MWW interlayer distance (nm); vertical layer alignment, bonding	MWW materials	MFI materials	Other zeolites
	3-D framework by direct synthesis;layers fused congruent.	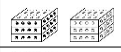	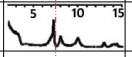	3 peaks	2.5 – not expanded; aligned and fused, continuous in 3D	MCM-49 As, calc	ZSM-5, silicalite-1	>230 frameworks
	Pseudo-ordered multi-layered precursor →ordered 3D structure	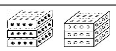	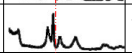	4 peaks	>2.6 - expanded; aligned; H-bond connected	MCM-22P/22	-	>15 frameworks
	Partly-ordered multi-layered → incomplete or disordered	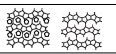	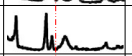	2 peaks +broad at 9°	>2.6 - expanded; shifted 1/3x+2/3y; H-bond connected	SSZ-70; ICNP-5	-	FER (ECR-12) NSI (EU-20)
	Disordered multi-layered → disordered	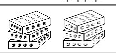	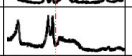	2 peaks +broad at 8-10°	>2.6 - expanded, misaligned; H-bond connected	EMM-10P/10; UZM-8	-	-
	Disordered mono-layered (unilamellar); delaminated,	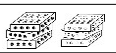	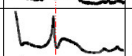	1 peak +broad at 8-10°	2.5 - not expanded; unaligned; not connected	MCM-56	-	-
	Multi-layered with surfactant (single-unit-cell nanosheets)		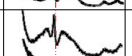	2 peaks, +broad at 8-10°	>2.6 - expanded, misaligned; organic lined	**UJM-1P/1 NEW**	Multilamellar nanosheets	-
	Mono-layered with surfactant; house-of-cards		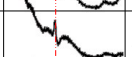	1 peak +broad at 8-10°	2.5; random layers - intergrown organic lined	MIT-1	Unilamellar nanosheets	-
	Self-pillared				MFI – intergrown at 90°	None	Self-pillared MFI-MEL	-

The proposed structures are idealised models and in the case of MWW are consistent with the observed XRD features. They are effectively end-members, while in practice formation of mixture is likely and is to be expected. On the other hand conditions for producing fairly pure phases are known. The proposed rationalization for the MWW family is qualitative and self-consistent but alternative explanations are not ruled out. Calculations of XRD patterns for mixtures of ordered and randomly dis-ordered layers in plane were carried out[33] confirming some the experimentally observed features, bud did not considered the expanded materials.

UJM-1P and MIT-1 as new types of MWW materials

UJM-1P and MIT-1 show XRD patterns qualitatively similar to EMM-10P and MCM-56 but can be counted as distinct 6th and 7th MWW representatives forming by direct synthesis. This is

justified by their formal similarity to the MFI analogues, i.e. being composed of the particular type of building units – layers with embedded bifunctional surfactant SDAs. This may be revised in the future but so far there are no well-defined or formal criteria for distinguishing/classifying various new layered materials and structures. Qualitative XRD differentiation seems inadequate in this situation when little is known about layered zeolites in general so additional factors can be considered and greater latitude for interpretation should be allowed. In, addition, as described below, both of these materials show some unique properties, especially with regard to layer disorder and swelling capacity, which further justifies separate treatment until all MWW species are better characterised.

It should be mentioned that other materials equivalent to EMM-1oP/-10 were reported with other SDAs and include: IPC-3P,[34] ITQ-30,[35] and hexamethonium MCM-22.[36] There is a report of direct synthesis of a swollen MWW material with mono-layers separated by surfactant with interlayer distance of ca 2 nm.[37] However, the preparation entails dissolution of another MWW material (ITQ-1) as substrate so it is not strictly a genuine one-pot preparation from scratch, but a 2-step procedure, so it will not be considered for now. MWW material denoted DS-ITQ-2 similar to MIT-1 has been also reported.[38]

UJM-1P structure and its formation from MIT-1

Based on the XRD pattern shown in Figure 3, and by comparison to MCM-22P the as-synthesised UJM-1P is identified as disordered (unaligned vertically) multi-layered MWW zeolite with expanded interlayer spacing, around >2.6 nm, revealed by the (002) reflection at ca 6.5° 2-θ. In short, it is roughly like the 'layered MWW precursor' MCM-22P but with disordered layer stacking. Based on the reported model for MIT-1, the layers are assumed to be lined with organic parts of the SDAs resulting in greater lateral disorder and easier swelling (vide supra) in comparison to the other multilayered expanded MWW (MCM-22P, EMM-10P). Just like the latter it also contracts to ca. 2.5 nm repeat upon calcination. The broad band at 8-10° 2-θ remains with no dip in the middle indicating preservation of the original layer stacking disorder.[24]

UJM-1P is obtained from the mono-layered MIT-1, which has XRD pattern similar to MCM-56. MIT-1 shown here has a small, broad peak around 6.5° 2-θ reminiscent of the (002) reflection present in as-synthesised multilayered MWW zeolites. It is unlikely an inherent feature of MIT-1 because simulations of the XRD patterns of MWW single-layer have no such feature,[20] nor is it seen with MCM-56. It should be assumed that this is an emerging peak due to the onset of UJM-1P formation. The conversion of MIT-1, which is apparently an intergrowth of mono-layers, to UJM-1P occurs most likely by recrystallization and not by layer restacking. It resembles the transition from MCM-56 to MCM-49, see Fig. 2, with some differences. The latter is a transition from mono-layers to complete 3D framework, while MIT-1 converts not into a framework but the multi-layered expanded product UJM-1P. It can be again attributed to the bulky SDAs preventing framework propagation in the 3rd dimension.

UJM-1P vs. the MFI analogue

The present material UJM-1P is considered to be an analogue of the multi-layered MFI[16] because of similarly designed template resulting in similar 'layer-with-surfactant' building blocks. There are differences between them, which is appropriate to discuss now. There are vastly different interlayer distances in UJM-1P and layered MFI, i.e. 0.2 nm vs. 2-4 nm, respectively. The former is comparable to the other layered MWW precursors (MCM-22P, EMM-10P). In MIT-1 the adamantyl groups were proposed[20] to fit in the surface pockets while the tails were lining the surface. This explains small layer separation in UJM-1P compared to MFI but must also entail lower organic content. This is indeed the case as UJM-1P contains about 30% organic and has shorter tail (C-16) than the MFI analogues (~45% organic and C-22). Elemental analysis of UJM-1P indicated partial degradation of the template (C/N ratio 13.5 vs. 17 calculated), which is common in hydrothermal syntheses with quaternary ammonium compounds. This also indicates that the real MIT-1 and UJM-1P may be somewhat different from the proposed models in terms of template location and distribution. The suggested location of adamantyl groups was inside the MWW surface pockets (cavities) but as they are neutral and hydrophobic they cannot serve as counterions to acidic Al sites. Does it mean there is not Al in these cavities or something else can balance them? This question remains open and may need further study.

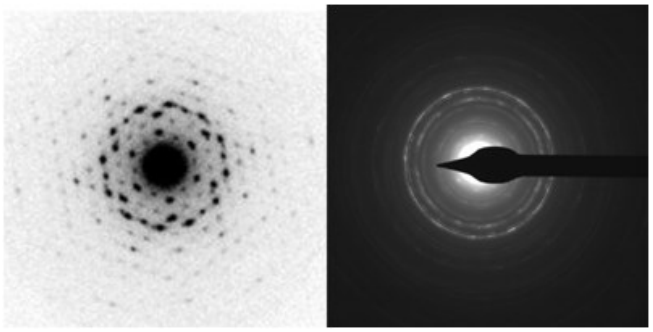

Figure 4. SAED patterns of EMM-10[24] and UJM-1P (uncalcined). Additional images are included in ESI.

TEM imaging and SAED of layer disorder

SAED patterns (Fig. 4) and TEM images (in ESI) for UJM-1P show significant lateral disorder. They are basically hexagonal but with extensive scatter of spots around the points outlining the hexagon. This significant lateral disorder is probably due lining of the layers with parts of the template extending from the pores to the surface. The available images of calcined EMM-10 indicate disorder as well but much less extensive.[24]

The majority phase shows disordered hexagonal electron diffraction patterns typical for MWW crystals viewed face-on, but with arcing indicative of layer misalignment, e.g. of the turbostratic nature. These differences between UJM-1P and EMM-10P may be due to particular samples that were tested and in the future may turn out to be less pronounced. This may be resolved as more information on more representatives of both materials becomes available.

Swelling with cationic surfactants

This is a standard tool for proving layered nature of layered materials and to obtain pillared materials.[6] The swelling of layered zeolites generally requires high pH such but differences can be observed when using surfactant hydroxide or surfactant salt plus NaOH.[39] For MCM-22P swelling with the latter was poor. MCM-56 was swollen with both media, and this was construed as indicating its better internal accessibility and easier layer separability due to loose mono-layered nature. The behaviour of UJM-1P is closer to MCM-56, see Table 2. In fact it showed the most facile swelling of all MWW materials so far. It is judged based on the relative intensity of the (003) reflection at ca. 5.5 deg, which is empirically established as a unique feature arising upon swelling of MWW materials.[40, 41] It is reflected in the patterns shown in Fig 5.

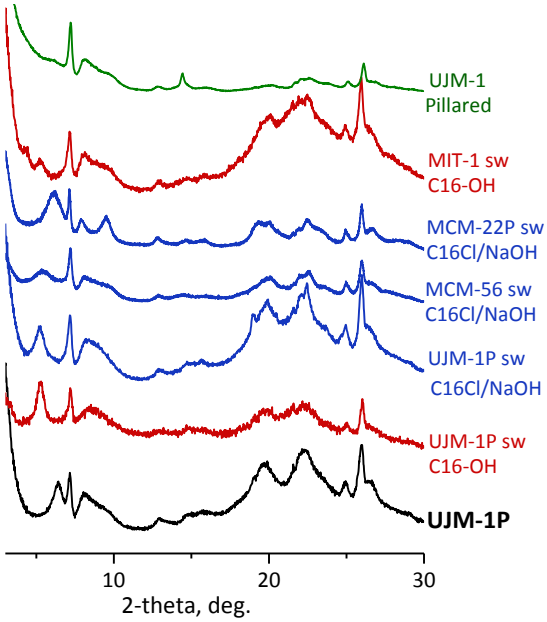

Figure 5. XRD pattern of layered MWW materials after swelling with HDTMA with hydroxide (C16-OH) and with chloride and NaOH (C16Cl-NaOH).

The lack of swelling of MCM-22P treated with HDTMA-Cl/NaOH is indicated by the (002) peak at >6° 2-θ and 2 separated peaks at ~8 and 10° 2-θ. We recognize that other factors may influence this intensity as well as the extent of swelling, which may depend for example on incidental layer intergrowth. Nonetheless UJM-1P is the best so far and a new benchmark thus may be viewed as attractive for layer manipulation/swelling/delamination with high efficiency. MIT-1 showed poor swelled even with the surfactant hydroxide, which confirms significant intergrowths within the house-of-cards' architecture.

Low angle (oo1) peaks at ca. 5 nm d-spacing are also observed (see SI) for swollen MWW structures but their intensity is sensitive to many factors so it is less reliable for quantitative estimation. Additional validation of swelling is based on pillaring and textural properties of the product. In the case of UJM-1P the pillared product showed greatly enhanced BET and pore volume, shown in Table 3, consistent with high degree of expansion and pillaring. The capacity of UJM-1P for facile swelling, even with HDTMA-Cl/NaOH, and formation of highly porous pillared structures, indicates overall weak layer connection, probably because of its unique structure.

Table 2. Swelling of layered MWW materials with cationic surfactants and different OH sources.

	Swelling solution	
MWW material	HTMA-OH	HDTMA-Cl+NaOH
MCM-22P	Yes	No
MCM-56	Yes	Yes
UJM-1P	Yes	Yes
MIT-1	No	n/a

Physical and catalytic properties of UJM-1

UJM-1 was characterised by nitrogen sorption at 77K, FTIR with pyridine adsorption (the data are presented in Table 2.) and in model catalytic reaction (mesitylene alkylation with benzyl alcohol, Figure 6.) to establish its basic properties in comparison to other MWW materials.

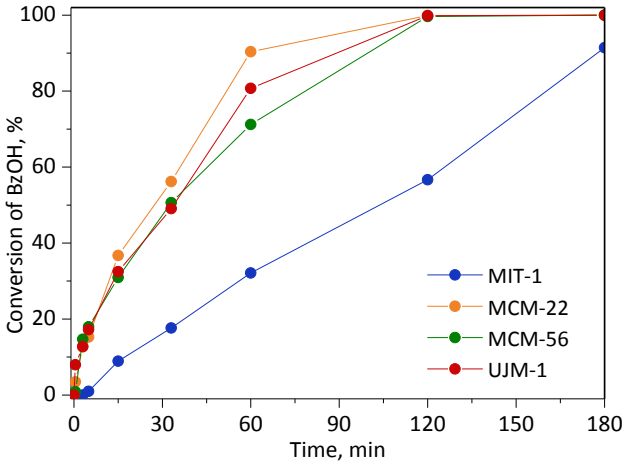

Figure 6. Benzyl alcohol conversions in reaction of mesitylene alkylation.

Both the textural and acid concentration characteristics of UJM-1 should be viewed as similar to MCM- 22 and MCM-56 despite numerical differences.[28, 42] They may be real but MWW materials are very sensitive to activation and post-synthesis treatments. To establish intrinsic activity differences may require elaborate testing. The acid site concentration in MIT-1 and pillared UJM-1 are viewed as really lower and fully justifiable with the latter due to the presence of inert silica

pillars. The low value of MIT-1 may be caused by many factors such the sample not being fully crystalline, more degraded during processing because of mono-layer nature and even this may be the property of MIT-1 that not all Al becomes acidic as described for MCM-56. The reported catalytic activity of MIT-1[20] was higher per active centre than MCM-22 and MCM-56. In our tests, shown in Fig. 6, it was less active than the other MWW materials, which again could be due to lower sample quality.

UJM-1 showed high activity that was comparable to MCM-22 and MCM-56. We will not judge these MWW materials as has been done in the past to show beneficial effects of expansion and openness on catalytic activity. There are many factors in such appraisal, many unknown and nothing short of dedicated systematic study can provide conclusive answers. For now we can only treat it on an individual basis (reactions) and hope that a coherent picture will emerge. As a new material easy to exfoliate and with surface lined with organics UJM-1P is an attractive candidate for controlled drug delivery studies.[43]

Table 3. Comparison of the properties of UJM-1 with selected MWW materials with different layered structure.

Zeolite	Si/Al, XRF	Si/Al(IR) BAS+LAS	Si/AL BAS	BAS(IR) µmol/g	LAS(IR) µmol/g	S_{BET} m^2/g	S_{out} m^2/g	V_{micro} cm^3/g	V_{meso} cm^3/g
MIT-1	18	45	53	307	55	500	240	0.086	0.02
UJM-1	18	16	18	899	86	500	135	0.114	0.03
MCM-56	8	14	15	1028	114	474	140	0.119	0.02
MCM-22 (24)	16	24	31	599	67	375	76	0.109	0.01
UJM-1 (pillared)	21	45	53	307	57	1063	154	0.322	0.09

Conclusions

In this paper, we present a new multilamellar MWW zeolite – UJM-1P – that has been obtained from the mono-layered MIT-1 by one-pot synthesis. The distinct X-Ray diffraction pattern of UJM-1P has confirmed its individual MWW layered structure with disordered stacking and expanded interlayer spacing (>2.6 nm). This type of zeolitic architecture was described before for the MFI topology as a multi-layered structure with surfactant (with single-unit-cell-thick nanosheets).

UJM-1 has relatively high concentration of Brønsted acid sites (about 900 µmol/g), BET area of about 500 m^2/g with preservation of microporosity (0.114 cm^3/g) which altogether makes it interesting material for catalysis. Moreover, the use of unusual, adamantyl-containing structure directing agent provides that the UJM-1P zeolite exhibits weak interlayer interaction, thus open architecture highly desirable for catalytic reaction with bulky molecules. The catalytic activity of the calcined form (UJM-1) was examined in the mesitylene alkylation with benzyl alcohol. The results showed conversions of benzyl alcohol comparable to other MWW family members: MCM-22 and MCM-56. The catalytic activity of UJM-1 was significantly higher than their unilamellar form – MIT-1.

The novel MWW layered zeolite architecture is interesting from the very fundamental point of view, nevertheless, the catalytic properties together with relatively simple (one-pot) way of synthesis make UJM-1P and its calcined form good candidates for further study towards scale-up and possible use of this material for the drug delivery industrial applications.

Conflicts of interest

There are no conflicts to declare.

Acknowledgements

Authors would like to acknowledge: National Science Center Poland grant no 2014/15/B/ST5/ 04498 (JG, WR, BG, AK); OP VVV "Excellent Research Teams", project No. CZ.02.1.01/ 0.0/0.0/15_003/0000417 – CUCAM (M.M., J.Č.); EPSRC grant EP/K025112/1 and Capital for Great Technologies grant EP/L017008/1 (M.M.); Czech Science Foundation P106/12/G015 (J.Č.). We thank Dr. D.N. Miller for help with the TEM and SAED.

References

1. J. Čejka, A. Corma and S. I. Zones, eds., *Zeolites and Catalysis: Synthesis, Reactions and Applications*, Wiley, 2010.
2. A. F. Masters and T. Maschmeyer, *Micropor. Mesopor. Mater.*, 2011, **142**, 423-438.
3. I. Fechete, Y. Wang and J. C. Védrine, *Catal. Today*, 2012, **189**, 2-27.
4. J. Weitkamp and L. Puppe, eds., *Catalysis and Zeolites: Fundamentals and Applications*, Springer, Berlin, 1999.
5. M. E. Leonowicz, J. A. Lawton, S. L. Lawton and M. K. Rubin, *Science*, 1994, **264**, 1910-1913.
6. W. J. Roth, C. T. Kresge, J. C. Vartuli, M. E. Leonowicz, A. S. Fung and S. B. McCullen, *Stud. Surf. Sci. Catal.*, 1995, **94**, 301-308.
7. L. Schreyeck, P. Caullet, J. C. Mougenel, J. L. Guth and B. Marler, *Microporous Materials*, 1996, **6**, 259-271.

8. W. J. Roth and D. L. Dorset, *Microporous Mesoporous Mater.*, 2011, **142**, 32-36.
9. J. V. Smith, *Chem. Rev.*, 1988, **88**, 149-182.
10. W. J. Roth, B. Gil and B. Marszalek, *Catal. Today*, 2014, **227**, 9-14.
11. W. J. Roth, B. Gil, W. Makowski, B. Marszalek and P. Eliasova, *Chem. Soc. Rev.*, 2016, **45**, 3400-3438.
12. W. J. Roth, P. Nachtigall, R. E. Morris and J. Čejka, *Chem. Rev.*, 2014, **114**, 4807–4837.
13. B. Marler and H. Gies, *European Journal of Mineralogy*, 2012, **24**, 405-428.
14. M. Mazur, P. S. Wheatley, M. Navarro, W. J. Roth, M. Položij, A. Mayoral, P. Eliášová, P. Nachtigall, J. Čejka and R. E. Morris, *Nat. Chem.*, 2016, **8**, 58-62.
15. P. Eliášová, M. Opanasenko, P. S. Wheatley, M. Shamzhy, M. Mazur, P. Nachtigall, W. J. Roth, R. E. Morris and J. Čejka, *Chem. Soc. Rev.*, 2015, **44**, 7177-7206.
16. M. Choi, K. Na, J. Kim, Y. Sakamoto, O. Terasaki and R. Ryoo, *Nature*, 2009, **461**, 246-U120.
17. K. Na, C. Jo, J. Kim, K. Cho, J. Jung, Y. Seo, R. J. Messinger, B. F. Chmelka and R. Ryoo, *Science*, 2011, **333**, 328-332.
18. K. Na, W. Park, Y. Seo and R. Ryoo, *Chemistry of Materials*, 2011, **23**, 1273-1279.
19. K. Na, M. Choi, W. Park, Y. Sakamoto, O. Terasaki and R. Ryoo, *Journal of the American Chemical Society*, 2010, **132**, 4169-4177.
20. H. Y. Luo, V. K. Michaelis, S. Hodges, R. G. Griffin and Y. Román-Leshkov, *Chemical Science*, 2015, **6**, 6320-6324.
21. T. F. Degnan, Jr., C. M. Smith and C. R. Venkat, *Applied Catalysis, A: General*, 2001, **221**, 283-294.
22. S. L. Lawton, A. S. Fung, G. J. Kennedy, L. B. Alemany, C. D. Chang, G. H. Hatzikos, D. N. Lissy, M. K. Rubin, H. K. C. Timken, S. Steuernagel and D. E. Woessner, *J. Phys. Chem.*, 1996, **100**, 3788-3798.
23. W. J. Roth and D. L. Dorset, *Micropor. Mesopor. Mater.*, 2011, **142**, 32-36.
24. W. J. Roth, D. L. Dorset and G. J. Kennedy, *Microporous and Mesoporous Materials*, 2011, **142**, 168-177.
25. R. H. Archer, J. R. Carpenter, S. J. Hwang, A. W. Burton, C. Y. Chen, S. I. Zones and M. E. Davis, *Chem. Mater.*, 2010, **22**, 2563-2572.
26. J. Čejka, W. J. Roth and M. Opanasenko, in *Comprehensive Supramolecular Chemistry II*, eds. G. W. Gokel, L. Barbour and J. L. Atwood, Elsevier Science, 2017, vol. 7, ch. 7.18, pp. 475-501.
27. S. I. Zones, *Microporous and Mesoporous Materials*, 2011, **144**, 1-8.
28. B. Gil, B. Marszalek, A. Micek-Ilnicka and Z. Olejniczak, *Top. Catal.*, 2010, **53**, 1340-1348.
29. S. Smeets, Z. J. Berkson, D. Xie, S. I. Zones, W. Wan, X. D. Zou, M. F. Hsieh, B. F. Chmelka, L. B. McCusker and C. Baerlocher, *J. Am. Chem. Soc.*, 2017, **139**, 16803-16812.
30. T. Moteki, W. Chaikittisilp, A. Shimojima and T. Okubo, *J. Am. Chem. Soc.*, 2008, **130**, 15780-15781.
31. X. Y. Zhang, D. X. Liu, D. D. Xu, S. Asahina, K. A. Cychosz, K. V. Agrawal, Y. Al Wahedi, A. Bhan, S. Al Hashimi, O. Terasaki, M. Thommes and M. Tsapatsis, *Science*, 2012, **336**, 1684-1687.
32. M. Opanasenko, W. Roth and J. Cejka, *Catal. Sci. Technol.*, 2016, **6**, 2742-2753.
33. M. Položij, H. V. Thang, M. Rubeš, P. Eliášová, J. Čejka and P. Nachtigall, *Dalton Trans.*, 2014, **43**, 10443-10450.
34. M. Kubů, W. J. Roth, H. F. Greer, W. Zhou, R. E. Morris, J. Přech and J. Čejka, *Chem. Eur. J.*, 2013, **19**, 13937-13945.
35. A. Corma, M. J. Diaz-Cabanas, M. Moliner and C. Martinez, *J. Catal.*, 2006, **241**, 312-318.
36. S. Goergen, E. Fayad, S. Laforge, P. Magnoux, L. Rouleau and J. Patarin, *Journal of Porous Materials*, 2011, **18**, 639-650.
37. L. Xu, X. Ji, S. Li, Z. Zhou, X. Du, J. Sun, F. Deng, S. Che and P. Wu, *Chem. Mater.*, 2016, **28**, 4512-4521.
38. V. J. Margarit, M. E. Martinez-Armero, M. T. Navarro, C. Martinez and A. Corma, *Angew. Chem. Int. Ed.*, 2015, **54**, 13724-13728.
39. W. J. Roth and J. C. Vartuli, *Stud. Surf. Sci. Catal.*, 2002, **141**, 273-279.
40. S. Maheshwari, E. Jordan, S. Kumar, F. S. Bates, R. L. Penn, D. F. Shantz and M. Tsapatsis, *Journal of the American Chemical Society*, 2008, **130**, 1507-1516.
41. W. J. Roth, J. Čejka, R. Millini, E. Montanari, B. Gil and M. Kubu, *Chem. Mater.*, 2015, **27**, 4620-4629.
42. B. Gil, W. Makowski, B. Marszalek, W. J. Roth, M. Kubu, J. Čejka and Z. Olejniczak, *Dalton Trans.*, 2014, **43**, 10501-10511.
43. G. Wyszogrodzka, P. Dorożyński, B. Gil, W. J. Roth, M. Strzempek, B. Marszałek, W. P. Węglarz, E. Menaszek, W. Strzempek and P. Kulinowski, *Pharmaceutical Research*, 2018, **35**.